

Randomized Functional Sparse Tucker Tensor for Compression and Fast Visualization of Scientific Data

P. Rai · H. Kolla · L. Cannada · A. Gorodetsky

Received: date / Accepted: date

Abstract We propose a strategy to compress and store large volumes of scientific data represented on unstructured grids. Approaches utilizing tensor decompositions for data compression have already been proposed. Here, data on a structured grid is stored as a tensor which is then subjected to appropriate decomposition in suitable tensor formats. Such decompositions are based on generalization of singular value decomposition to tensors and capture essential features in the data with storage cost lower by orders of magnitude. However, tensor based data compression is limited by the fact that one can only consider scientific data represented on structured grids. In case of data on unstructured meshes, we propose to consider data as realizations of a function that is based on functional view of the tensor thus avoiding such limitations. The key is to efficiently estimate the parameters of the function whose complexity is small compared to the cardinality of the dataset (otherwise there is no compression). Here, we introduce the set of functional sparse Tucker tensors and propose a method to construct approximation in this set such that the resulting compact functional tensor can be rapidly evaluated to recover the original data. The compression procedure consists of three steps. In the first step, we consider a fraction of the original dataset for interpolation on a structured grid followed by sequentially truncated higher order singular value decomposition to get a compressed version of the interpolated data. We then fit singular vectors on a set of functional basis using sparse approximation to obtain corresponding functional sparse Tucker tensor representation. Finally, we re-evaluate the coefficients of this functional tensor using randomized least squares at a reduced computational complexity. This strategy leads to compression ratio of orders of magnitude on combustion simulation datasets.

Keywords Data compression, Functional tensors, Tucker decomposition, Sparse approximations, Randomized least squares

P.Rai, H. Kolla, L. Cannada
Sandia National Laboratories, Livermore, USA
Correspondence E-mail: pmrai@sandia.gov

A. Gorodetsky
Aerospace Engineering, University of Michigan, Ann Arbor, USA

1 Introduction

Functional tensors are based on interpretation of high dimensional functions as tensors and their decomposition in several tensor formats as particular approximations. Consequently, functional tensors have been studied and applied for sampling based approximation of high dimensional functions in cases where the number of available function evaluations is small. Several functional tensor formats have been studied for various applications e.g. [14] [11][19] [18]. These approaches rely on linearity between the parameters of the low-rank format and the output of the function. Utilizing this multilinear parameterization, they convert the low-rank function approximation to one of low-rank tensor decomposition for the coefficients of a tensor-product basis.

The novelty of the present paper, in contrast, is aimed at detecting low rank structure in the large volumes of data in order to obtain a low complexity functional tensor representation for a small loss in accuracy. As opposed to high dimensional function approximation using tensors in earlier works, high dimensionality does not come from the number of function parameters but from the number of data points required to be processed in order to obtain a functional tensor form. This functional tensor, stored as a surrogate at a fraction of cost of the original dataset, can be rapidly evaluated to recover accurate approximations of the data. The compressed functional form can act as a preview of the full dataset, which may reside on long-term storage and need not replace the original dataset. In this paper, we consider a particular type of tensor format i.e. functional sparse Tucker representation of the data noting that the ideas presented here can be readily extended to other tensor formats.

Several compression methods largely focus on compressing local structure with very little loss in precision. Examples of such methods include multivariate volume block data reduction by taking advantage of local multiway structure [17], compression of data in local blocks [23,12]. Tensor based methods, in contrast, aim at detecting global structure in the data. It does not process the data in blocks but rather considers the data in its entirety. In this work, in order to take advantage of tensor based compression, we first interpolate the unstructured data on a structured grid followed by its Tucker decomposition [27]. Singular vectors with truncated rank for each mode thus obtained are represented as functions on a suitable basis using least squares with sparsity constraints thus resulting in a functional sparse Tucker representation of the dataset. Finally, to compensate for the effect of interpolation of data for Tucker compression, we re-estimate the components of the core tensor, at a much lower computation complexity than classical approaches, by solving a randomized least squares problem using data in the original dataset.

The manuscript is organized as follows. We introduce and formalize the notion of functional sparse Tucker tensors in section 2. In order to construct approximations in this set, we review least squares with sparse regularization in section 3. We then present our construction algorithm in section 4 and apply a randomized method for re-estimation of core tensor in section 5. Finally, we illustrate our results on combustion simulation datasets in section 6 with a short conclusion in section 7.

2 Functional Sparse Tucker Tensors

The key idea in this work is to represent the dataset as realizations of a multivariate function

$$u(y_1, \dots, y_d) = \sum_{i_1=1}^{n_1} \cdots \sum_{i_d=1}^{n_d} \beta_{i_1, \dots, i_d} \phi_{i_1}^{(1)}(y_1) \cdots \phi_{i_d}^{(d)}(y_d),$$

where $\phi_{i_k}^{(k)}, 1 \leq k \leq d$ are basis functions (e.g. polynomials, wavelets...). The number of expansion coefficients β_{i_1, \dots, i_d} are $\prod_{k=1}^d n_k$ thus manifesting the curse of dimensionality if n_k or d or both are large. In such cases, we instead represent the data as realizations of a Tucker low rank approximation \tilde{u} of u where

$$\tilde{u}(y_1, \dots, y_d) = \sum_{j_1=1}^{r_1} \cdots \sum_{j_d=1}^{r_d} \alpha_{j_1, \dots, j_d} w_{j_1}^{(1)}(y_1) \cdots w_{j_d}^{(d)}(y_d). \quad (1)$$

Storage of \tilde{u} in (1) require $\prod_{k=1}^d r_k$ coefficients and $\sum_{k=1}^d n_k r_k$ expansion coefficients of $w_{j_k}^{(k)}(y_k), 1 \leq j_k \leq r_k, 1 \leq k \leq d$ such that

$$w_{j_k}^{(k)}(y_k) = \sum_{i_k=1}^{n_k} w_{i_k, j_k}^k \phi_{i_k}^{(k)}(y_k). \quad (2)$$

In additional, in order to gain advantage from sparsity based regularization, we also constraint the number of non zero coefficients in (2). In the following, we formalize the notion of functional sparse Tucker tensors.

We introduce approximation spaces $\mathcal{S}_{n_k}^k$ with orthonormal basis $\{\phi_j^{(k)}\}_{j=1}^{n_k}$, such that

$$\begin{aligned} \mathcal{S}_{n_k}^k &= \left\{ v^{(k)}(y_k) = \sum_{j=1}^{n_k} v_j^k \phi_j^{(k)}(y_k); v_j^k \in \mathbb{R} \right\} \\ &= \left\{ v^{(k)}(y_k) = \phi^{(k)}(y_k)^T \mathbf{v}^{(k)}; \mathbf{v}^{(k)} \in \mathbb{R}^{n_k} \right\}, \end{aligned}$$

where $\mathbf{v}^{(k)}$ denotes the vector of coefficients of $v^{(k)}$ and where $\phi^{(k)} = (\phi_1^{(k)}, \dots, \phi_{n_k}^{(k)})^T$ denotes the vector of basis functions. An approximation space $\mathcal{S}_{\mathbf{n}}$ is then obtained by tensorization of approximation spaces $\mathcal{S}_{n_k}^k$:

$$\mathcal{S}_{\mathbf{n}} = \mathcal{S}_{n_1}^1 \otimes \cdots \otimes \mathcal{S}_{n_d}^d = \left\{ v = \sum_{i \in I_{\mathbf{n}}} v_i \phi_i; v_i \in \mathbb{R} \right\},$$

where $I_{\mathbf{n}} = \times_{k=1}^d \{1 \dots n_k\}$ and $\phi_i(y) = (\phi_{i_1}^{(1)} \otimes \cdots \otimes \phi_{i_d}^{(d)})(y_1, \dots, y_d) = \phi_{i_1}^{(1)}(y_1) \cdots \phi_{i_d}^{(d)}(y_d)$. An element $v = \sum_i v_i \phi_i \in \mathcal{S}_{\mathbf{n}}$ can be identified with the algebraic tensor $\mathbf{v} \in \mathbb{R}^{n_1} \otimes \cdots \otimes \mathbb{R}^{n_d}$ such that $(\mathbf{v})_i = v_i$. Denoting $\phi(y) = \phi^{(1)}(y_1) \otimes \cdots \otimes \phi^{(d)}(y_d) \in \mathbb{R}^{n_1} \otimes \cdots \otimes \mathbb{R}^{n_d}$, we have the identification $\mathcal{S}_{\mathbf{n}} \simeq \mathbb{R}^{n_1} \otimes \cdots \otimes \mathbb{R}^{n_d}$ with

$$\mathcal{S}_{\mathbf{n}} = \{v(y) = \langle \phi(y), \mathbf{v} \rangle; \mathbf{v} \in \mathbb{R}^{n_1} \otimes \cdots \otimes \mathbb{R}^{n_d}\},$$

where $\langle \cdot, \cdot \rangle$ denotes the canonical inner product in $\mathbb{R}^{n_1} \otimes \cdots \otimes \mathbb{R}^{n_d}$.

Here, we suppose that the approximation space $\mathcal{S}_{\mathbf{n}}$ is sufficiently rich to allow accurate representations of a large class of functions (e.g. by choosing polynomial spaces with high degree, wavelets with high resolution...). We now introduce the set of functional sparse tensors.

Let \mathcal{R}_1 denote the set of (elementary) rank-one tensors in $\mathcal{S}_{\mathbf{n}} = \mathcal{S}_{n_1}^1 \otimes \dots \otimes \mathcal{S}_{n_d}^d$, defined by

$$\mathcal{R}_1 = \left\{ w(y) = \left(\bigotimes_{k=1}^d w^{(k)} \right) (y) = \prod_{k=1}^d w^{(k)}(y_k) ; w^{(k)} \in \mathcal{S}_{n_k}^k \right\},$$

or equivalently by

$$\mathcal{R}_1 = \left\{ w(y) = \langle \phi(y), \mathbf{w}^{(1)} \otimes \dots \otimes \mathbf{w}^{(d)} \rangle ; \mathbf{w}^{(k)} \in \mathbb{R}^{n_k} \right\},$$

where $\phi(y) = \phi^{(1)}(y_1) \otimes \dots \otimes \phi^{(d)}(y_d)$, with $\phi^{(k)} = (\phi_1^{(k)}, \dots, \phi_{n_k}^{(k)})^T$ the vector of basis functions of $\mathcal{S}_{n_k}^k$, and where $\mathbf{w}^{(k)} = (w_1^k, \dots, w_{n_k}^k)^T$ is the set of coefficients of $w^{(k)}$ in the basis of $\mathcal{S}_{n_k}^k$, that means $w^{(k)}(y_k) = \sum_{i=1}^{n_k} w_i^k \phi_i^{(k)}(y_k)$. Correspondingly, we define \mathbf{m} -sparse rank-one subset defined as

$$\mathcal{R}_1^{\mathbf{m}\text{-sparse}} = \left\{ w(y) = \langle \phi(y), \mathbf{w}^{(1)} \otimes \dots \otimes \mathbf{w}^{(d)} \rangle ; \mathbf{w}^{(k)} \in \mathbb{R}^{n_k}, \|\mathbf{w}^{(k)}\|_0 \leq m_k \right\}$$

with effective dimension $\sum_{k=1}^d m_k \ll \sum_{k=1}^d n_k$ (here we only count the values of the non-zero coefficients and not the integers indicating their locations). However performing least-squares approximation in this set may not be computationally tractable. We thus introduce a convex relaxation of the ℓ_0 -“norm” to define the subset \mathcal{R}_1^γ of \mathcal{R}_1 defined as

$$\mathcal{R}_1^\gamma = \left\{ w(y) = \langle \phi(y), \mathbf{w}^{(1)} \otimes \dots \otimes \mathbf{w}^{(d)} \rangle ; \mathbf{w}^{(k)} \in \mathbb{R}^{n_k}, \|\mathbf{w}^{(k)}\|_1 \leq \gamma_k \right\},$$

where the set of parameters $(\mathbf{w}^{(1)}, \dots, \mathbf{w}^{(d)})$ is now searched in a convex subset of $\mathbb{R}^{n_1} \times \dots \times \mathbb{R}^{n_d}$.

Finally, we introduce the set of functional Tucker tensors with multilinear Tucker rank $\mathbf{r} = (r_1, \dots, r_d)$

$$\mathcal{T}_{\mathbf{r}} = \left\{ v = \sum_{j_1=1}^{r_1} \dots \sum_{j_d=1}^{r_d} \alpha_{j_1, \dots, j_d} w_{j_1, \dots, j_d} ; w_{j_1, \dots, j_d} \in \mathcal{R}_1 \right\}$$

and the corresponding sparse subset

$$\mathcal{T}_{\mathbf{r}}^\gamma = \left\{ v = \sum_{j_1=1}^{r_1} \dots \sum_{j_d=1}^{r_d} \alpha_{j_1, \dots, j_d} w_{j_1, \dots, j_d} ; w_{j_1, \dots, j_d} \in \mathcal{R}_1^\gamma \right\}.$$

In the following, we propose algorithms for the construction of approximations in tensor subsets $\mathcal{T}_{\mathbf{r}}^\gamma$ which requires sparse approximation of functions $w_{j_k}^k(y_k)$. For this purpose, we use least squares with sparse regularization as described in the next section.

3 Least squares with sparse regularization

A sparse function is one that can be represented using few non zero terms when expanded on a suitable basis. In general, a successful reconstruction of sparse solution vector depends on sufficient sparsity of the coefficient vector and additional properties (incoherence) depending on the samples and of the chosen basis (see [7, 13]). More precisely, an approximation $\sum_{i=1}^P v_i \phi_i(y)$ of a function $u(y)$ is considered as sparse on a particular basis $\{\phi_i(y)\}_{i=1}^P$ if it admits a good approximation with only a few non zero coefficients. Under certain conditions, a sparse approximation can be computed accurately using only $Q \ll P$ samples of $u(y)$ via sparse regularization. Given the random samples $\mathbf{z} \in \mathbb{R}^Q$ of the function $u(y)$ at sample points $\{y^q\}_{q=1}^Q$, a best m -sparse (or m -term) approximation of u can be ideally obtained by solving the constrained optimization problem

$$\min_{\mathbf{v} \in \mathbb{R}^P} \|\mathbf{z} - \Phi \mathbf{v}\|_2^2 \quad \text{subject to} \quad \|\mathbf{v}\|_0 \leq m, \quad (3)$$

where $\|\mathbf{v}\|_0 = \#\{i \in \{1, \dots, P\} : v_i \neq 0\}$ is the so called ℓ_0 -“norm” of \mathbf{v} which gives the number of non zero components of \mathbf{v} and $\Phi \in \mathbb{R}^{Q \times P}$ the matrix with components $(\Phi)_{q,i} = \phi_i(y^q)$. Problem (3) is a combinatorial optimization problem which is NP hard to solve. Under certain assumptions, problem (3) can be reasonably well approximated by the following constrained optimization problem which introduces a convex relaxation of the ℓ_0 -“norm”:

$$\min_{\mathbf{v} \in \mathbb{R}^P} \|\mathbf{z} - \Phi \mathbf{v}\|_2^2 \quad \text{subject to} \quad \|\mathbf{v}\|_1 \leq \delta, \quad (4)$$

where $\|\mathbf{v}\|_1 = \sum_{i=1}^P |v_i|$ is the ℓ_1 -norm of \mathbf{v} . Since the ℓ_2 and ℓ_1 -norms are convex, we can equivalently consider the following convex optimization problem, known as Lasso [26] or basis pursuit [10]:

$$\min_{\mathbf{v} \in \mathbb{R}^P} \|\mathbf{z} - \Phi \mathbf{v}\|_2^2 + \lambda \|\mathbf{v}\|_1, \quad (5)$$

where $\lambda > 0$ corresponds to a Lagrange multiplier whose value is related to δ . Problem (5) appears as a regularized least-squares problem. The ℓ_1 -norm is a sparsity inducing regularization function in the sense that the solution \mathbf{v} of (5) may contain components which are exactly zero. Several optimization algorithms have been proposed for solving (5) (see [3]). In this paper, we use the Lasso modified least angle regression algorithm (see LARS presented in [16]) and fast leave-one-out cross validation error estimate [8] for optimal sparse solution (corresponding to regularization parameter λ) which relies on the use of the Sherman-Morrison-Woodbury formula (see [6] for its implementation within Lasso modified LARS algorithm). In this work, we have used Lasso modified LARS implementation of SPAMS software [24] for ℓ_1 -regularization.

4 Functional Sparse Tucker Using TuckerMPI

4.1 Interpolation on structured grid

Representation of the dataset in functional sparse Tucker format defined in section 2 requires estimation of the core tensor α and univariate functions $w_j^{(k)}(y_k)$. If the

dataset is available on a structured grid, it can be stored as a tensor \mathcal{U} which can then be decomposed in Tucker format

$$\mathcal{U} \approx \tilde{\mathcal{U}} = \boldsymbol{\alpha} \times_1 W^{(1)} \times_2 W^{(2)} \dots \times_d W^{(d)},$$

where \times_k is mode k product of \mathcal{U} with a factor matrix $W^{(k)} \in \mathbb{R}^{n_k \times r_k}$. Here, the compression precision is given by

$$\epsilon = \frac{\|\mathcal{U} - \tilde{\mathcal{U}}\|_F}{\|\mathcal{U}\|_F},$$

where $\|\cdot\|_F$ is the Frobenius norm. Since the dataset considered is unstructured, we propose to interpolate the data on a structured grid. Let us denote the grid size in mode k , $1 \leq k \leq d$ as I_k and, for the sake of simplicity, consider that the grid points are equispaced. A structured grid of size $I_1 \times I_2 \dots \times I_d$ can thus be obtained. Now, we consider only a small subset of the original dataset, say 10%, for linear interpolation on this grid and the interpolated data is stored as a tensor which is then decomposed in Tucker format. We use TuckerMPI [4], a parallel C++/MPI software package for compressing distributed data, for this purpose. Note that TuckerMPI is a parallel implementation of the sequentially-truncated HOSVD (ST-HOSVD) [28]. We thus obtain factor matrices $W^{(k)}$, $1 \leq k \leq d$, the columns of which are realizations of univariate functions $w_{j_k}^{(k)}(y_k)$, $1 \leq j \leq r_k$.

4.2 Sparse approximation of singular vectors

We now wish to obtain a functional representation $w_{j_k}^{(k)}(y_k)$, $1 \leq j_k \leq r_k$, of the singular vectors $W_{:,j_k}^{(k)}$ such that $W_{i_k,j_k}^{(k)}$ are evaluations of $w_{j_k}^{(k)}(y_k^{i_k})$ at grid locations $\{y_k^{i_k}\}_{i_k=1}^{I_k}$ along mode k . For this purpose, we use least squares with sparse regularization in section 3 to obtain coefficients on suitable basis functions. It is well known that singular vectors are more oscillatory (see for e.g. Figure 3(a)) for higher rank as they capture high frequency phenomenon in the dataset. Thus, choice of basis functions for representation of $w_{j_k}^{(k)}(y_k)$ corresponding to small j_k may not be appropriate for the ones with higher j_k . Therefore, in this work, we propose to construct approximation in two spaces \mathbb{P}_p , where \mathbb{P}_p is the space of Legendre polynomials of degree p and $\mathbb{W}_{s,p}$, where $\mathbb{W}_{s,p}$ is the space of multi-resolution wavelets with resolution s and degree p . We can then choose the approximation that gives smaller approximation error. We present the overall compression scheme in Algorithm 1 below.

5 Re-estimation of core tensor using randomized least squares

Algorithm 1 gives a functional representation of the data in the sparse Tucker format. The data however was interpolated on a structured grid to be able to use TuckerMPI for obtaining the singular vectors. This approach suffers from the limitation that the quality of approximation will depend on the type of interpolation (e.g. linear, non linear interpolation, cardinality of points considered for interpolation etc.) on a structured grid. To overcome this limitation, it is imperative to

Algorithm 1 Compression of unstructured data in functional sparse Tucker format

Input: Original dataset, interpolation grid $I_k, 1 \leq k \leq d$, compression precision ϵ
Output: Function sparse Tucker tensor core α and coefficients of $w_{j_k}^{(k)}(y_k), 1 \leq k \leq d, 1 \leq j_k \leq r_k$.

- 1: Interpolate the data on structured grid of size $I_1 \times \cdots \times I_d$
 - 2: Use TuckerMPI to get core tensor α and factor matrices $W^{(k)}$ for given compression precision
 - 3: **for** $k = 1, \dots, d$ **do**
 - 4: **for** $j_k = 1, \dots, r_k$ **do**
 - 5: Approximate $w_{j_k}^{(k)}$ using components of $W_{:,j_k}^{(k)}$ in \mathbb{P}_p and $\mathbb{W}_{s,p}$ and estimate error (See section 3)
 - 6: Store coefficients of $w_{j_k}^{(k)}$ corresponding to smaller approximation error
 - 7: **end for**
 - 8: **end for**
-

use the original dataset to re-evaluate some, if not all, parameters of functional sparse Tucker tensor. We implement this idea by re-evaluating the elements of the core tensor using linear least squares. Let us rewrite (1) as

$$u(y) = \tilde{u}(y) = \sum_{j=1}^R \alpha_j w_j(y),$$

where $\mathbf{j} = (j_1, \dots, j_d)$ such that $\alpha_j = \alpha_{j_1, \dots, j_d}$ and $w_j(y) = \prod_{k=1}^d w_{j_k}^{(k)}(y_k)$ and $R = r_1 \times \cdots \times r_d$. We wish to solve the regression problem

$$\hat{\alpha} = \min_{\alpha \in \mathbb{R}^R} \|\mathbf{u} - \mathbf{W}\alpha\|_2^2, \quad (6)$$

where $(\mathbf{u})_q = u(y^q)$, $\mathbf{W} \in \mathbb{R}^{Q \times R}$ is the matrix such that $(\mathbf{W})_{q,j} = w_j(y^q)$ and $\alpha \in \mathbb{R}^R$ are components of the core tensor reshaped as a vector. Clearly, \mathbf{W} is overdetermined ($Q \gg R$), and hence its computation and storage may be prohibitive in the considered setting. However, sketching and randomized methods have been used successfully to solve big linear least squares problems at a much smaller computation cost [25, 15, 2, 21] and is ideal for application in this setting.

The key here is to transform (6) using random projection $\mathbf{M} \in \mathbb{R}^{S \times R}, S \ll Q$, such that an exact solution to $\min_{\alpha} \|\mathbf{M}\mathbf{u} - \mathbf{M}\mathbf{W}\alpha\|_2^2$ is an approximate solution to the original problem (6) [29]. Approaches to solve randomized least squares problems are based on the idea of leverage scores. The leverage score of rows of \mathbf{W} is the norm of the rows of its left singular vectors and corresponds, in some sense, to the importance of that row in constructing its column-space. One can then solve the randomized least squares problem by sampling rows of \mathbf{W} weighted according to the distribution of the leverage scores. One drawback of this method is that leverage scores have to be estimated from singular value decomposition of \mathbf{W} which may be computationally expensive when R is large. Therefore, we follow the approach in [5], where we mix \mathbf{W} with the intention of evenly distributing leverage scores across all rows in such a way that one can sample rows uniformly. Note that this mixing strategy relates to a more general class of transformations that rely on approximation quality guarantees provided by the Johnson-Lindenstrauss Lemma [20]. This lemma specifies a class of random projections that preserve the distances between all pairs of vectors with reasonable accuracy in the projected subspace.

We briefly summarize steps for our problem. Firstly, we premultiply \mathbf{W} by a diagonal matrix $\mathbf{D} \in \mathbb{R}^{Q \times Q}$ with random $+1/-1$ to spread out the signal in frequency domain [1]. This is equivalent to flipping the sign of each row of \mathbf{W} with probability $1/2$. We then apply a fast mixing operation, here a fast Fourier transformation, which has the effect of mixing information across every element of a vector. At the end of this step, the leverage scores of the resulting matrix are concentrated about a small value. Finally, we sample S rows of this matrix with uniform probability. These steps define the random projection \mathbf{M} . Algorithm 2 outlines the steps in re-estimation of the core tensor.

Algorithm 2 Re-evaluation of the core tensor using Randomized Least Squares

Input: Original dataset \mathbf{u} , Core tensor α , Functional singular vectors $w_{j_k}^{(k)}, 1 \leq k \leq d, 1 \leq j_k \leq r_k$
Output: Re-evaluated Function sparse Tucker tensor core $\hat{\alpha}$
1: Construct \mathbf{W} by evaluating w_j at samples in the dataset
2: Multiply \mathbf{W} and \mathbf{u} with diagonal matrix \mathbf{D}
3: Apply a fast Fourier Transformation i.e. $\mathcal{F}\mathbf{D}\mathbf{W}$ and $\mathcal{F}\mathbf{D}\mathbf{u}$
4: Sample $S > R$ rows uniformly, i.e. $\mathbf{S}\mathcal{F}\mathbf{D}\mathbf{W}$ and $\mathbf{S}\mathcal{F}\mathbf{D}\mathbf{u}$, where \mathbf{S} is a sampling matrix
5: Solve $\hat{\alpha} = \min_{\alpha} \|\mathbf{S}\mathcal{F}\mathbf{D}\mathbf{W} - \mathbf{S}\mathcal{F}\mathbf{D}\mathbf{u}\|_2^2$

6 Illustration

We apply our compression strategy on a data set pertaining to a direct numerical simulation (DNS) of turbulent combustion. A “statistically planar” (SP) premixed flame [22] stabilized in homogeneous isotropic turbulence is simulated using the massively parallel DNS code S3D [9]. A premixed mixture of methane and air establish a flame that remains statistically planar and stationary in an oncoming turbulent flow. The combustion chemistry is described using a chemical mechanism containing six chemical species. Accordingly, at each point in the spatial grid and time the solution vector contains eleven dependent variables describing the full thermo-chemical state of the flame. The data set is mapped onto a 3-dimensional structured grid comprising 500 grid points in each spatial dimension, and a total of 400 time snapshots are considered. For the illustration of the method, to follow, we consider two variants of this fundamentally 4-dimensional data set. In the first case, henceforth referred to as SP3D, we consider that the data belongs to a three dimensional space, consisting of two spatial axis and one time axis. The total number of data points in this set is 7.5×10^7 with total storage cost of 0.6 gigabytes for double precision. The second case considers a 4 order tensor, SP4D, which also considers the third spatial axis, in addition to the ones in SP3D. The total storage cost of data in this case is 300 gigabytes with 3.75×10^{10} data points. In the following, we illustrate results of SP3D case, and mention that a similar illustrations can be obtained for SP4D.

In case of SP3D, we interpolate the data on a structured grid of size $500 \times 500 \times 300$ using only 10% of the data in the original set and decompose the resulting tensor in Tucker format using TuckerMPI. Figure 1 shows the decay in the absolute value of the components of the core tensor α versus rank (multilinear

Tucker rank on horizontal axis is converted to canonical rank) of SP3D for Tucker decomposition precision of 1.0×10^{-4} . We clearly see that there is a fast decay in the singular values thus indicating strong scope for compressibility of this dataset. Table 1 summarizes the interpolation parameters and multilinear Tucker ranks i.e. size of the core tensor thus obtained for different decomposition precisions for the two datasets.

Table 1 Specification of interpolation grid size and Tucker ranks obtained for different precision using TuckerMPI for two test cases

Dataset	Interpolation grid size	Precision (ϵ)	Size of core tensor
SP3D	$500 \times 500 \times 300$	1.0×10^{-2}	$25 \times 24 \times 8$
		1.0×10^{-4}	$57 \times 50 \times 17$
SP4D	$500 \times 500 \times 500 \times 300$	1.0×10^{-2}	$30 \times 38 \times 5 \times 11$

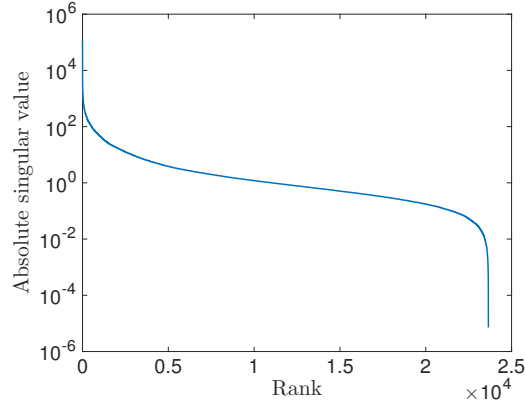


Fig. 1 Decay of singular values i.e. absolute value of components of core tensor α v/s rank of SP3D with TuckerMPI precision of 1.0×10^{-4} . The rank on horizontal axis is converted to canonical rank by sorting the singular values in descending order.

We now consider functional approximations of singular vectors along the first mode. Figure 2(a) shows first singular vector $W_{:,1}^{(1)}$ and its corresponding functional approximations in \mathbb{P}_{20} and \mathbb{P}_{40} . For better illustration, the corresponding approximation errors are plotted in Figure 2(b). We find that a sufficiently rich approximation space is necessary for accurate representation of singular vectors as point wise error for $p = 40$ is much smaller than with $p = 20$.

Figure 3(a) and (b) show similar plots for the last singular vector in the first mode i.e. $W_{:,57}^{(1)}$ in approximation spaces \mathbb{P}_{40} and $\mathbb{W}_{3,5}$. We clearly see that, in this case, a multi-resolution wavelet basis is essential to get an accurate functional representation, although point wise approximation error is high as compared to the first singular vector. This is because the singular vectors corresponding to higher ranks capture high frequency signals in the dataset and hence require functional basis with higher resolution.

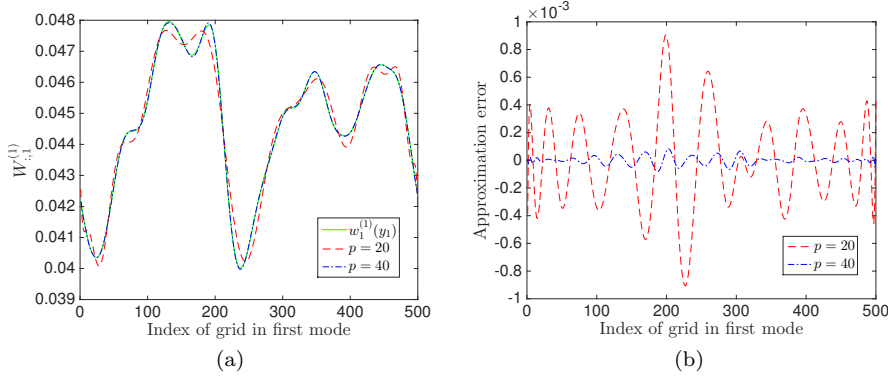


Fig. 2 (a) Approximation of $w_1^{(1)}(y_1)$ using least squares with ℓ_1 regularization from data points as components of $W_{:,1}^{(1)}$ in the approximation space of Legendre polynomials of degree $p = 20$ and $p = 40$. (b) Point wise approximation error v/s grid index of the two approximations in (a)

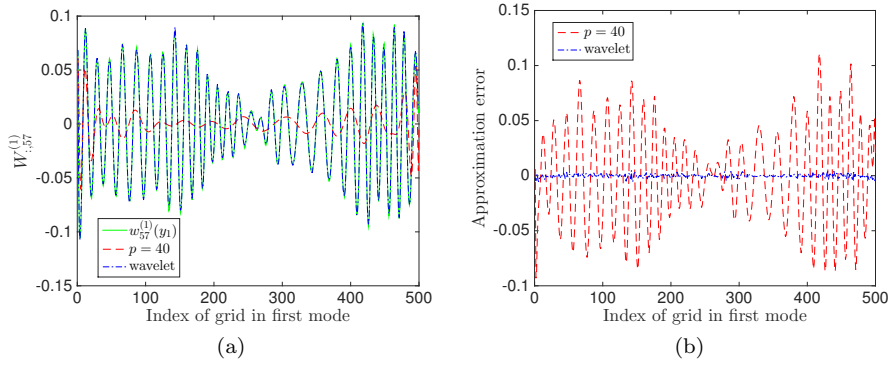


Fig. 3 Approximation of $w_{57}^{(1)}(y_1)$ using least squares with ℓ_1 regularization from data points as components of $W_{:,57}^{(1)}$ in the approximation space of Legendre polynomials of degree $p = 20$ and wavelets with resolution level 5 and degree 3. (b) Point wise approximation error v/s grid index of the two approximations in (a)

We now illustrate results related to re-estimation of core tensor using randomized least squares. In Figure 4, we show the distribution of the leverage score of the measurement matrix \mathbf{W} (see section 5) before and after mixing operation (Step 3. of algorithm 2). We find that leverage scores, although skewed, have non negligible mass in the range of $[0.2, 0.5]$. On the other hand, after application of mixing operation, leverage scores are concentrated around a small value (0.12). One can thus sample the desired number of rows uniformly to reduce the size of problem (6). In Figure 5, we illustrate self convergence of the re-estimated core tensor by measuring the relative norm of change in α (by solving step 5. of algorithm 2) for $S = S_1$ and $S = S_2$, where $S_2 > S_1$. We find two distinct regions in the plot separated by a sharp drop in self convergence error at $S \approx 2.5R$. Here $R = 25 \times 24 \times 8$, i.e. size of the core tensor whose coefficients are being re-estimated. Note that an

oversampling factor of 2.5 is orders of magnitude smaller as compared to size of the problem when estimating the core tensor with all points in the dataset.

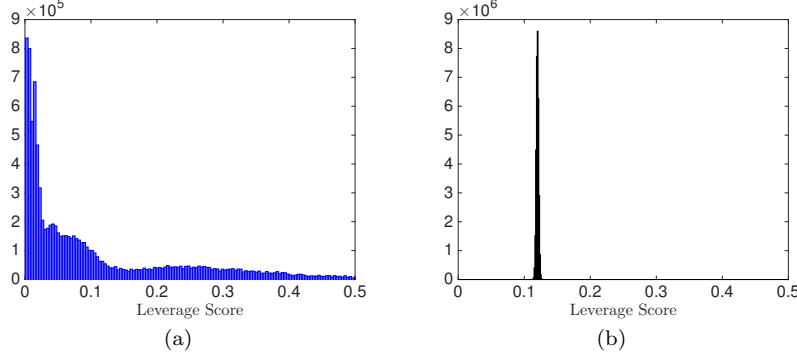


Fig. 4 Histogram plot of leverage scores of the measurement matrix \mathbf{W} in (a) before mixing and (b) after mixing (Step 3. of Algorithm 2)

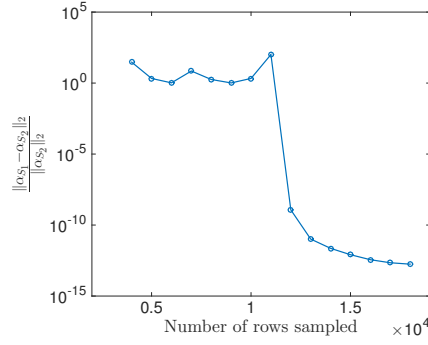


Fig. 5 Self convergence plot of α . Horizontal axis shows the number of rows S sampled in Step 4. of algorithm 2. Vertical axis shows the change in α (relative norm) estimated by sampling S_1 and S_2 rows ($S_2 = S_1 + 10^3, S_1 \in \{3000, 4000, \dots, 17000\}$).

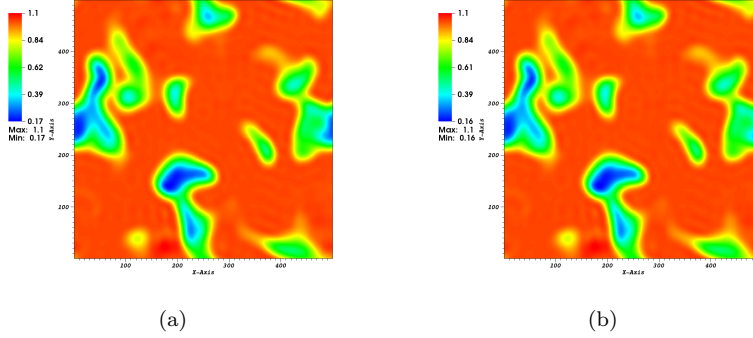
Table 2 shows compression error, compression ratio and storage cost for functional sparse Tucker tensor for both test cases. Finally, Figure 6 shows visualization of 2D slice of the original dataset obtained from reconstruction of data from sparse functional Tucker tensor. Note that reconstruction of the data from functional tensor is computationally inexpensive as the only computation required is evaluation of the basis functions at points of interest.

7 Conclusion

We presented a novel technique to compress large volume of data using functional sparse Tucker decomposition. The key idea is to find a sufficiently accurate repre-

Table 2 Compression results using functional sparse Tucker tensor

Dataset	Original Storage cost	Precision	Compression ratio	Reduced Storage cost
SP3D	0.6 GB	1.01×10^{-2}	3879	155 KB
		1.9×10^{-4}	936	640 KB
SP4D	300 GB	1.1×10^{-2}	4.45×10^5	673 KB

**Fig. 6** Visualization of a 2D slice of SP4D dataset. (a) Original data and (b) Reconstructed tensor slice obtained from randomized functional sparse Tucker tensor.

sensation of data in the set of functional Tucker tensors with complexity smaller by orders of magnitude as compared to the size of dataset. In order to achieve this objective, we defined the set of sparse functional Tucker tensors and used existing parallel implementation of Tucker decomposition to construct approximation in this set. The singular vectors are approximated as functions represented on suitable basis using least squares with sparse regularization. The entire compression scheme was tested on datasets obtained from high fidelity combustion modeling simulations. For small loss of accuracy, the proposed strategy results in compression ratio of up to $10^3 - 10^5$ for a third order and fourth order dataset respectively.

8 Acknowledgment

We would like to acknowledge Tamara Kolda for discussions related to this work. Sandia National Laboratories is a multimission laboratory managed and operated by National Technology and Engineering Solutions of Sandia, LLC., a wholly owned subsidiary of Honeywell International, Inc., for the U.S. Department of Energy's National Nuclear Security Administration.

References

1. Nir Ailon and Bernard Chazelle. Approximate nearest neighbors and the fast johnson-lindenstrauss transform. In *Proceedings of the thirty-eighth annual ACM symposium on Theory of computing*, pages 557–563. ACM, 2006.
2. Haim Avron, Petar Maymounkov, and Sivan Toledo. Blendenpik: Supercharging lapack's least-squares solver. *SIAM Journal on Scientific Computing*, 32(3):1217–1236, 2010.

3. Francis Bach, Rodolphe Jenatton, Julien Mairal, Guillaume Obozinski, et al. Optimization with sparsity-inducing penalties. *Foundations and Trends® in Machine Learning*, 4(1):1–106, 2012.
4. Grey Ballard, Alicia Klinvex, and Tamara G Kolda. Tuckermppi: A parallel c++/mpi software package for large-scale data compression via the tucker tensor decomposition. *arXiv preprint arXiv:1901.06043*, 2019.
5. Casey Battaglini, Grey Ballard, and Tamara G Kolda. A practical randomized cp tensor decomposition. *SIAM Journal on Matrix Analysis and Applications*, 39(2):876–901, 2018.
6. G. Blatman and B. Sudret. Adaptive sparse polynomial chaos expansion based least angle regression. *Journal of Computational Physics*, 230:2345–2367, 2011.
7. E. Candes, J. Romberg, and T. Tao. Near optimal signal recovery from random projections: Universal encoding strategies? *IEEE Transactions on information theory*, 52(12):5406–5425, 2006.
8. Gavin C Cawley and Nicola LC Talbot. Fast exact leave-one-out cross-validation of sparse least-squares support vector machines. *Neural networks*, 17(10):1467–1475, 2004.
9. J H Chen, A Choudhary, B de Supinski, M DeVries, E R Hawkes, S Klasky, W K Liao, K L Ma, J Mellor-Crummey, N Podhorszki, R Sankaran, S Shende, and C S Yoo. Terascale direct numerical simulations of turbulent combustion using s3d. *Computational Science & Discovery*, 2(1):015001, jan 2009.
10. Scott Shaobing Chen, David L Donoho, and Michael A Saunders. Atomic decomposition by basis pursuit. *SIAM review*, 43(1):129–159, 2001.
11. Mathilde Chevreuil, Régis Lebrun, Anthony Nouy, and Prashant Rai. A least-squares method for sparse low rank approximation of multivariate functions. *SIAM/ASA J. Uncertain. Quantif.*, 3(1):897–921, 2015.
12. Sheng Di and Franck Cappello. Fast error-bounded lossy hpc data compression with sz. In *2016 ieee international parallel and distributed processing symposium (ipdps)*, pages 730–739. IEEE, 2016.
13. David L Donoho et al. Compressed sensing. *IEEE Transactions on information theory*, 52(4):1289–1306, 2006.
14. Alireza Doostan, AbdoulAhad Validi, and Gianluca Iaccarino. Non-intrusive low-rank separated approximation of high-dimensional stochastic models. *Comput. Methods Appl. Mech. Eng.*, 263:42–55, 2013.
15. Petros Drineas, Michael W Mahoney, S Muthukrishnan, and Tamás Sarlós. Faster least squares approximation. *Numerische mathematik*, 117(2):219–249, 2011.
16. Bradley Efron, Trevor Hastie, Iain Johnstone, Robert Tibshirani, et al. Least angle regression. *The Annals of statistics*, 32(2):407–499, 2004.
17. Nathaniel Fout, Kwan-Liu Ma, and James Ahrens. Time-varying, multivariate volume data reduction. In *Proceedings of the 2005 ACM symposium on Applied computing*, pages 1224–1230. ACM, 2005.
18. Alex Gorodetsky, Sertac Karaman, and Youssef Marzouk. A continuous analogue of the tensor-train decomposition. *Computer Methods in Applied Mechanics and Engineering*, 347:59–84, 2019.
19. Alex A Gorodetsky and John D Jakeman. Gradient-based optimization for regression in the functional tensor-train format. *Journal of Computational Physics*, 374:1219–1238, 2018.
20. William B Johnson and Joram Lindenstrauss. Extensions of lipschitz mappings into a hilbert space. *Contemporary mathematics*, 26(189-206):1, 1984.
21. Ravindran Kannan and Santosh Vempala. Randomized algorithms in numerical linear algebra. *Acta Numerica*, 26:95–135, 2017.
22. H. Kolla, X.-Y. Zhao, N. Swaminathan, and J.H. CHen. Velocity and reactive scalar dissipation spectra in turbulent premixed flames. *Combustion Science and Technology*, 188(9):1424–1439, 2016.
23. Peter Lindstrom. Fixed-rate compressed floating-point arrays. *IEEE transactions on visualization and computer graphics*, 20(12):2674–2683, 2014.
24. Julien Mairal, Francis Bach, Jean Ponce, and Guillermo Sapiro. Online learning for matrix factorization and sparse coding. *Journal of Machine Learning Research*, 11(Jan):19–60, 2010.
25. Vladimir Rokhlin and Mark Tygert. A fast randomized algorithm for overdetermined linear least-squares regression. *Proceedings of the National Academy of Sciences*, 105(36):13212–13217, 2008.

-
26. Robert Tibshirani. Regression shrinkage and selection via the lasso. *Journal of the Royal Statistical Society: Series B (Methodological)*, 58(1):267–288, 1996.
 27. Ledyard R Tucker. Some mathematical notes on three-mode factor analysis. *Psychometrika*, 31(3):279–311, 1966.
 28. Nick Vannieuwenhoven, Raf Vandebril, and Karl Meerbergen. A new truncation strategy for the higher-order singular value decomposition. *SIAM Journal on Scientific Computing*, 34(2):A1027–A1052, 2012.
 29. David P Woodruff et al. Sketching as a tool for numerical linear algebra. *Foundations and Trends® in Theoretical Computer Science*, 10(1–2):1–157, 2014.